Food Chemistry: X 23 (2024) 101668

Contents lists available at ScienceDirect

Food Chemistry: X

journal homepage: www.sciencedirect.com/journal/food-chemistry-x

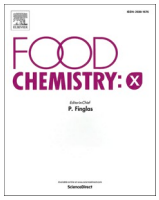

Dynamic profiling of metabolite changes and health-promoting functions in 'yuling paste' during nine steaming and nine sun-drying processes

Yue E [a,b], Weimiao Li [a], Hongbin Guo [b], Xianman Zhang [c], Qinggele Caiyin [a,*], Yi Yuan [a,*]

[a] School of Chemical Engineering and Technology, Tianjin University, Tianjin 300072, China
[b] Zhejiang Institute of Tianjin University, Shaoxing, 312300 Shaoxing, Zhejiang, China
[c] Zhejiang Zhongxin Fluoride Materials Co., Ltd, No. 5 North Thirteen Road, Shangyu, Shaoxing, Zhejiang, 312369, China

ARTICLE INFO

Keywords:
Yuling paste
Nine steaming nine sun-drying cycles
Active ingredients
Metabolite profile change
Health-promoting mechanism

ABSTRACT

Yuling paste, a traditional Chinese health food derived from longan pulp and American ginseng, undergoes a unique processing method involving nine cycles of steaming and sun-drying. Ultra-high-performance liquid chromatography tandem mass spectrometry combined with widely targeted metabolomics has been used to examine the dynamic change in metabolite profiles through the processing. A total of 758 metabolites were identified. Processing significantly affects metabolite changes, and network pharmacology is subsequently used to explore potential pharmacological ingredients. After processing, the contents of active ingredients such as ginsenoside rh2, oleanolic acid, choline, D-glucose, and D-galacturonic acid were found to increase significantly. These increases can be correlated to the enhancement of five distinct pathways, and the contents of naringenin-7-O-glucoside, adenosine, pantothenic acid, and D-sucrose decreased after the processing, correlating with decreases in two different pathways. This study provides a comprehensive reference and scientific basis for understanding the health benefits associated with this traditional health food.

1. Introduction

Yuling paste, a traditional Chinese functional food, is crafted from a blend of longan pulp and American ginseng in a weight ratio of 10:1 following a historical recipe documented in the 'Dietary Prescriptions for the Suixiju Retreat' by Qing Dynasty physician Wang Mengying (Yu, 2020). The book mentioned that Yuling paste has the effects of relieving insomnia, enhancing qi and nourishing blood as a traditional Chinese health food.

Longan pulp is the aril of the Sapindaceae plant *Dimocarpus longan* Lour (Tindall, 1994). This sub-tropical fruit tree is of significant importance in Southeast Asia and has been widely cultivated in many countries, including China, Thailand, Vietnam, India, Australia and parts of the subtropical regions of the United States (Zhang, Guo, Ho, & Bai, 2020a). In China, longan cultivation has a long history and is mainly distributed in Fujian, Guangxi, Guangdong, Sichuan, and other regions. Longan is rich in nutrients such as polysaccharides, polyphenols, flavonoids, lipids, saponins, peptides, amino acids, vitamins and various trace elements, which are beneficial to health (Zhang, Guo, Ho, & Bai, 2020b; Yang, Jiang, Shi, Chen, & Ashraf, 2011). Longan has a variety of biological activities, including antioxidant, immunomodulatory, anti-ageing, nervous system regulation and anti-tumour activities (Zhang et al., 2020a). Longan pulp polysaccharides have been found to have prebiotic activity and intestinal barrier protective properties (Bai et al., 2023). American ginseng (*Panax quinquefolius* L.) is a perennial herbaceous plant of the genus Panax of the ginsengaceae family, containing active ingredients such as saponins, flavonoids, polysaccharides and amino acids (Szczuka et al., 2019). Key health benefits of American ginseng include immune system enhancement (Kiefer & Pantuso, 2003), anti-cancer activity (Corbit, Ebbs, King, & Murphy, 2006), cognitive enhancement (Shin et al., 2016), and blood sugar regulation (Kan et al., 2017). Research indicates that the steaming process may alter or enhance certain medicinal properties of American ginseng, potentially increasing beneficial compounds or improving their bioavailability (Zheng et al., 2017).

'Nine steaming nine sun-drying', also known as 'nine steaming nine exposure', is a common food and herbal processing technology in ancient China (Cheng et al., 2021; Liao et al., 2022). The method involves repeating cycles of steaming and sun-drying up to nine times to maximise therapeutic effects while minimising toxic side effects. Many foods and medicinal materials are processed using this technique, including black sesame seeds (Cheng et al., 2021), black soybeans (Liao

* Corresponding authors.
E-mail addresses: qinggele@tju.edu.cn (Q. Caiyin), yuanyi@tju.edu.cn (Y. Yuan).

https://doi.org/10.1016/j.fochx.2024.101668
Received 23 April 2024; Received in revised form 15 July 2024; Accepted 16 July 2024
Available online 18 July 2024
2590-1575/© 2024 The Authors. Published by Elsevier Ltd. This is an open access article under the CC BY-NC-ND license (http://creativecommons.org/licenses/by-nc-nd/4.0/).

et al., 2022), rehmannia radix (Gong et al., 2021), polygonati rhizoma (Su et al., 2023; Zhu et al., 2022), polygonum (Sun et al., 2023), etc. The process of nine steaming and nine sun-drying has different effects on different foods and medicinal herbs, and it can reduce toxicity, improve taste and enhance or improve pharmacological activity. For example, the nine steaming and nine sun-drying process has a significant effect on the content and activity of the phenolic compounds in black soybeans. The antioxidant activity of in vitro digested black soybean products with an appropriate steaming and sun-drying degree is higher than that of raw black soybean (Liao et al., 2022). The process has a significant impact on the chemical composition of black sesame seeds. After evaporating to dryness, the total relative content of aldehydes in sesame increased, while the total relative content of hydrocarbons and esters decreased (Cheng et al., 2021). Interestingly, the process can also enhance the immune activity of some traditional Chinese medicinal herbals, such as polygonati rhizoma. The immunomodulatory activity of Polygonatum polysaccharide is enhanced after processing; the spleen and thymus indexes are significantly increased, and the expressions of IL-2, IFN-γ, IgA, IgM and the CD4+/CD8+ ratio are also increased at different steaming times (Su et al., 2023).

Although the nine steaming nine sun-drying 'Yuling paste' is widely consumed as a health food, the efficacy of this food is mainly based on traditional clinical experience and lacks a scientific and comprehensive theoretical basis. However, the process is complex and the optimum steaming and drying times are still controversial. There are few reports on the dynamic changes of active ingredients during the process as well as the mechanism of 'tonifying qi and nourishing blood'. Ultra-high-performance liquid chromatography tandem mass spectrometry (UPLC–MS/MS) coupled with widely targeted metabolomics has been used to examine the dynamic changes of metabolites during the nine steaming and nine sun-drying cycles. Network pharmacology has been used to explore the potential pharmacological ingredients and the mechanism of 'tonifying qi and nourishing blood'. In addition, changes in the primary active metabolites during the processing stages were carefully examined, and these results will provide a comprehensive reference and scientific basis for this healthy food.

2. Materials and methods

2.1. Experimental materials

Methanol (MeOH) and acetonitrile (ACN) were purchased from Merck (Darmstadt, Germany), and formic acid was purchased from Aladdin, All standard samples were purchased from Sigma-Aldrich. Yuling paste samples were kindly provided by Gui Yuan Tian Ju Jiu Zheng Jiu Zhi Fang, Yu Zhou City (Chinese Medicine Processing and Pharmaceutical Techniques of Yu Zhou, Intangible Cultural Heritage of Henan Province).

2.2. Steaming and sun-drying process

Put the longan arils and American ginseng powder into a pot and mix them in a weight ratio of 10:1. Place the pot over a wooden stove to steam for 12 h/day. After steaming, the mixture is to sun-dried for about 12 h, and the related procedure will be repeated for nine cycles. Six processed samples (labelled as 0–0, 1, 3, 5, 7 and 9) were collected each cycle.

2.3. Analysis of metabolites

2.3.1. Sample preparation and extraction

Biological samples are lyophilized through a vacuum freeze-dryer (Scientz-100F), and the freeze-dried samples are pulverized using a mixer mill (MM 400, Retsch) with zirconia beads for 1.5 min at 30 Hz. About 50 mg of the lyophilised powder was dissolved in a 1.2 mL 70% MeOH and vortexed for 30 s at 30 min intervals for a total of six times. After centrifugation at 12,000 rpm for 3 min, the extract was filtrated (SCAA-104, 0.22 μm pore size; ANPEL, Shanghai, China) and subjected to the UPLC-MS/MS analysis.

2.3.2. UPLC conditions

The prepared samples were analysed using a UPLC-ESI-MS/MS system (UPLC, SHIMADZU Nexera X2; MS, Applied Biosystems 4500 Q TRAP). The analysis conditions are as follows, UPLC: Agilent SB-C18 column (1.8 μm, 2.1 mm * 100 mm); the mobile phase: solvent A of pure water with 0.1% formic acid, solvent B of ACN with 0.1% formic acid. The analysis is performed using a gradient program: start with 95% A and 5% B, then gradient to 5% A and 95% B over 9 min, hold for 1 min, then gradient back to 95% A and 5.0% B over 1.1 min, and hold for 2.9 min. The flow rate is 0.35 mL /min, the column oven is 40 °C, and the injection volume is 4 μL.

2.3.3. ESI-QTRAP-MS/MS

ESI operation parameters are as follows: source temperature 550 °C, ion spray voltage 5500 V (positive mode)/−4500 V (negative mode), ion source gas I (50 psi), gas II (60 psi) and curtain gas (25 psi). MS instrument tuning and mass calibration were performed using 10 and 100 μmol/L polypropylene glycol solutions for QQQ and LIT modes, respectively. QQQ scans were acquired for the MRM experiments as the collision gas (nitrogen) set at medium. The declustering potential (DP) and collision energy (CE) of each MRM transition were determined by additional DP and CE optimizations. A set of MRM transitions were monitored based on the metabolites eluting during the experiment.

2.4. Statistical analysis

2.4.1. Principal component analysis

Unsupervised principal component analysis (PCA) was performed using the statistical function prcomp within R (www.r-project.org). Data were unit variance scaled before unsupervised PCA.

2.4.2. Hierarchical cluster analysis and Pearson correlation coefficients

Hierarchical cluster analysis (HCA) results for samples and metabolites are presented as heatmaps with dendrograms, but Pearson correlation coefficient (PCC) between samples is calculated using the cor function in R and presents only as a heatmap. HCA and PCC were performed using the R package Complex Heatmap. For HCA, normalized signal intensities (unit variance scaling) of metabolites are visualised as chromatograms.

2.4.3. Differential metabolites selected

For two-group analysis, differential metabolites were determined by VIP (VIP $\geq$ 1) and absolute Log2FC (|Log2FC| $\geq$ 1.0). VIP values were extracted from Orthogonal Projections of Latent Structures Discriminant Analysis (OPLS-DA) results, which contain score plots and permutation plots, and were generated using the R package MetaboAnalystR. Data were log-transformed and mean-centred before OPLS-DA, and permutation tests (200 permutations) were performed to avoid overfitting.

3. Results and discussion

3.1. Widely targeted metabolomic profiling

A total of 921 different metabolites were detected, including 156 lipids, 129 triterpenoids, 81 amino acids and their derivatives, 63 flavonoids, 141 phenolic acids, 54 nucleotides and their derivatives, 8 tannins, 67 alkaloids, 91 organic acids, 26 lignans and coumarins, and 104 unidentified compounds. Overlay analysis of the QC-TIC diagram (Fig. S1) showed that the data collected in this study had good reproducibility and reliability.

PCA distinguishes the original group from the treated group. Fig. 1a shows that the QC sample is highly concentrated, suggesting that the

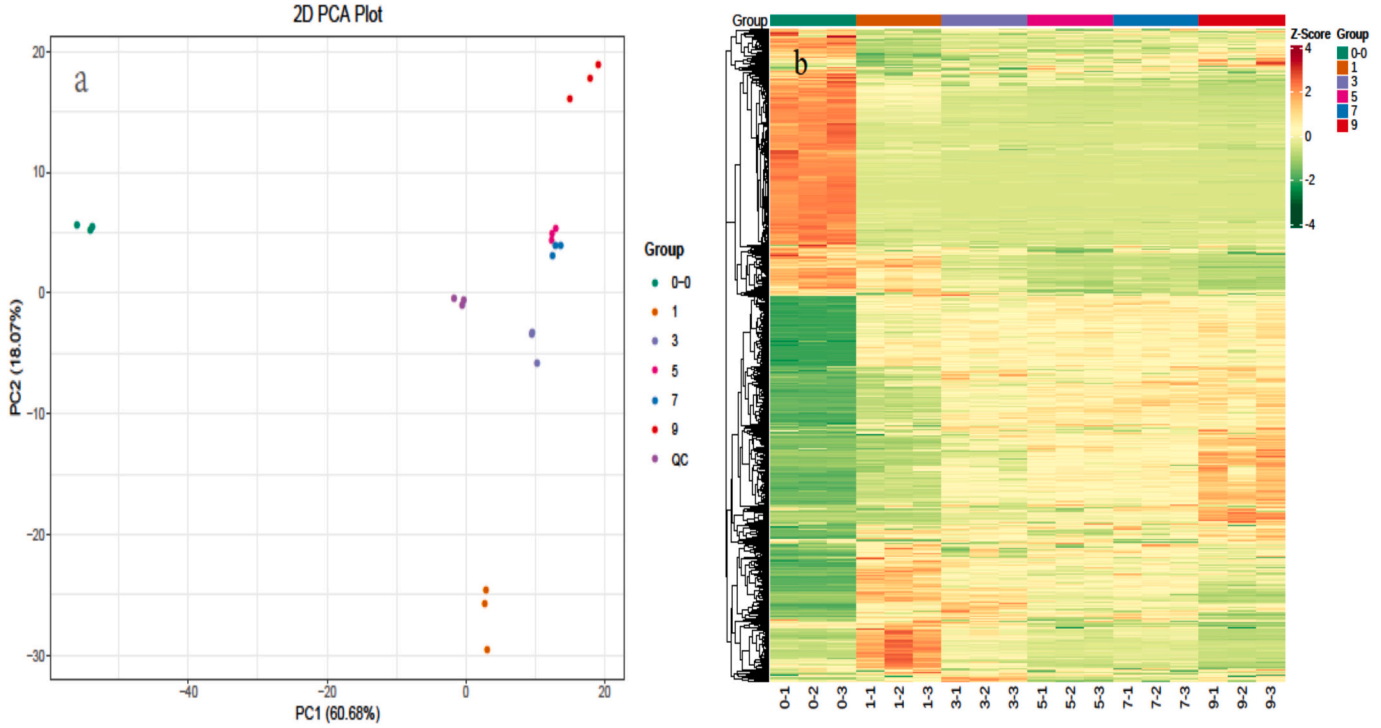

Fig. 1. PCA (a) and HCA (b) analyses of differential metabolites among the original group and the processed groups(0–0 represent the original group, 1–9 represent groups processed through cycles one to nine, respectively.).

analysis is robust and reproducible. The five-steaming five-drying and seven-steaming seven-drying groups overlap slightly without obvious separation. In contrast, the remaining groups were distributed in different regions, suggesting similar metabolites between the former two and differences in the latter. Hierarchical cluster analysis of metabolites during processing is shown in Fig. 1b. The HCA results show that except for overlap of the five-steaming five-drying and the seven-steaming seven-drying groups, the remaining groups are clearly differentiated, and the compositions of the parallel samples within the group are similar.

Orthogonal Projections to Latent Structures Discriminant Analysis (OPLS-DA) was performed to screen for different metabolites between the original and treated groups. The comparison between the original and the treated group obtained using the OPLS-DA model is shown in Fig. S2. The Q^2 values for all control groups exceeded 0.9, indicating that the model is stable and reliable.

To more clearly and visually represent the overall differences in metabolism, fold change (FC) values were calculated for metabolites in the comparison groups. These FC values are sorted in ascending order to generate a dynamic profile of differences in metabolite content. As shown in Fig. S3, the top 10 upregulated and downregulated metabolites were annotated.

3.2. Screening differential metabolites during processing

Differential metabolites were screened according to VIP >1, FC ≥ 2 or ≤ 0.5. Figs. 2a–e show volcano plots of metabolites between the original and the processed groups. In the comparison groups, 599 (0 vs. 1),617 (0 vs. 3), 644 (0 vs. 5), 638 (0 vs. 7) and 636 (0 vs. 9) metabolites were significantly different. For example, as shown in Fig. 2e, the metabolite volcano plot between the original and the nine steaming/nine drying groups identified 636 differential metabolites responsible for metabolic changes during processing. Compared with the original group, the total metabolites in the treated group shows a significant change: 353 compounds are upregulated and 283 compounds are downregulated.

The Venn diagram (Fig. 2f) shows that the presence of common and unique metabolites among the compared groups. Specifically, 496 common metabolites differed between the orignal and processed groups, confirming a significant effect of processing. Moreover, 25, 3, 10, 2, 18 unique metabolites were found in the 0 vs. 1, 0 vs.3, 0 vs.5, 0 vs.7 and 0 vs.9 processed groups, respectively. These results indicate that steaming and drying cycles lead to significant changes in metabolite profiles, and the steaming and drying processes may promote oxidation, hydrolysis together with other metabolite-alterin reactions.

To further characterize metabolite changes during processing, differential metabolites were classified into nine subcategories based on K-means clustering (Fig. 3). For example, in subcategories 1 and 8, the metabolite content generally shows a decreasing trend with increasing treatment cycles. The metabolite content in subcategories 4 and 6 shows an increasing trend with increasing treatment cycles. Interestingly, in subcategory 2, the metabolite content first decreases and then increases after the initial processing. But in subcategories 3, 5 and 9, metabolite content first increases after the initial processing and then decreases. Nevertheless, in subcategory 7, the metabolite content first decrease after the initial processing and then remains unchanged.

3.3. Dynamic changes in differential metabolites during processing

Differential metabolites were screened according to the criteria VIP >1, fold change ≥2 or ≤ 0.5. A total of 758 differential metabolites were identified, including 117 lipids, 121 triterpenes, 67 amino acids and their derivatives, 50 flavonoids, 115 phenolic acids, 49 nucleotides and their derivatives, 6 tannins, 57 alkaloids, 72 organic acids, 22 lignan coumarins and coumarins, together with 82 unidentified compounds. Among these compounds, 126 were detected only in the processed group (Table S1).

The FCs of differential metabolites were compared among the groups. Examination of Fig. 4 shows the top 20 metabolites with the highest FC for each set of comparisons, and the proportion of metabolites showing an upregulation trend gradually decreases as the processing cycle increases. As expected, the proportion of metabolites

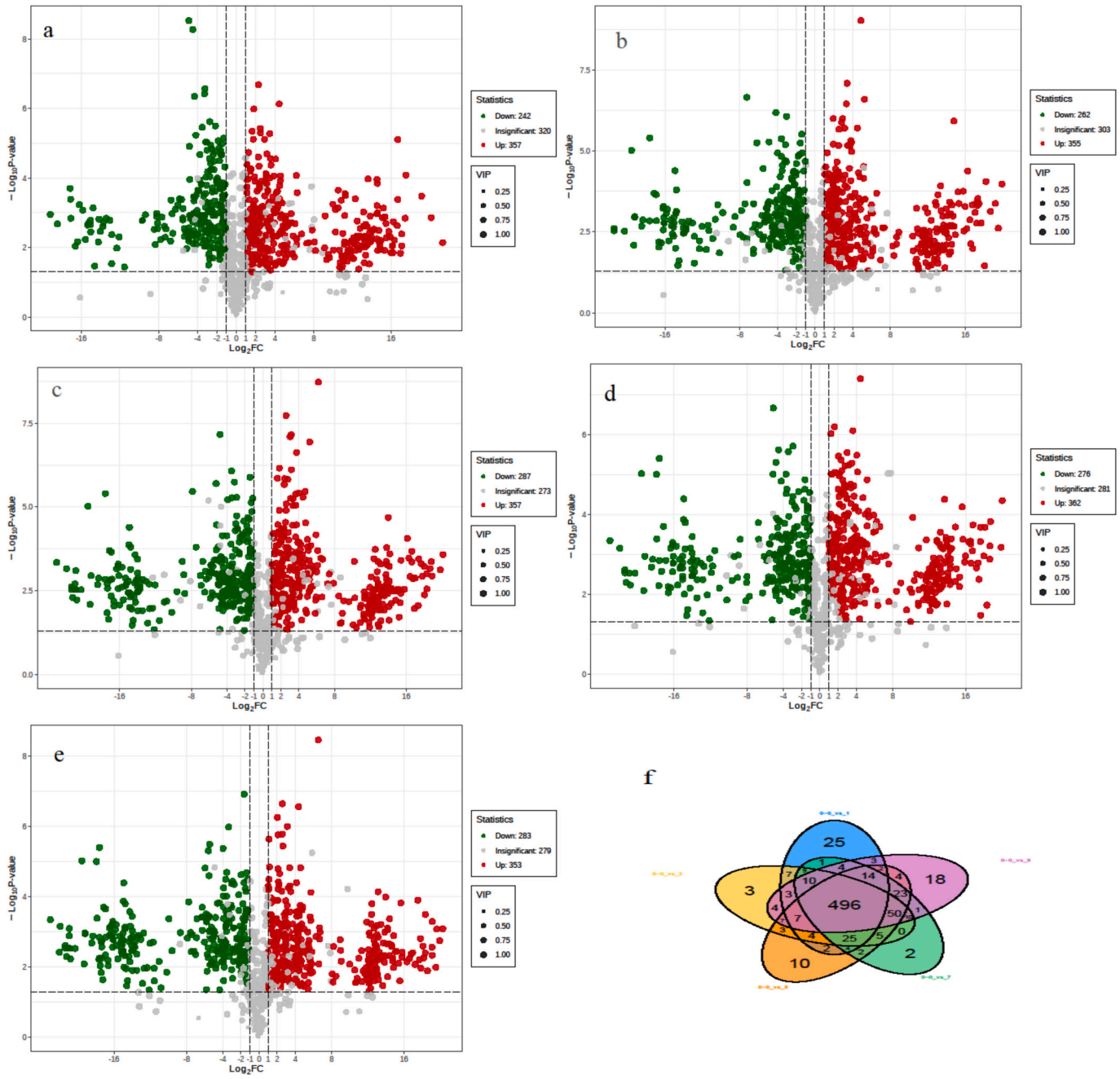

Fig. 2. Volcano plot (a-d) of the differential metabolites of original group vs processed groups. Venn diagram (f) of the differential metabolites of the original group vs. the processed groups. a.0 vs. 1, b. 0 vs. 3, c.0 vs. 5, d.0 vs. 7, e.0 vs. 9.

showing a downregulation trend increases, indicating that the treatment results in a significant change in metabolite numbers.

3.3.1. Phenolic compounds

Phenolic compounds are known for their powerful anti-oxidant property to scavenge free radicals. Also, phenolic compounds can inhibit enzymes responsible for generating reactive oxygen species (ROS), thereby reducing highly oxidizsed ROS species, effectively mitigating oxidative stress. Phenolics are the main chemical structures responsible for the antioxidant properties of longan fruits (Robards, Prenzler, Tucker, Swatsitang, & Glover, 1999; Zhang et al., 2018). Among the top 20 compounds (Fig. 4) with the highest FCs in different groups, phenolic compounds account for the highest proportion. For example, brevifolin carboxylic acid, phloroglucinol, and 5,7-dihydroxy-1(3H)-isobenzofuranone exhibit an uptrend after the processing. But 3-*O*-methylgallic acid, 6-O-galloyl-β-D-glucose, 1-O-galloyl-β-D-glucose, 4-aminobenzoic acid, 1-O-salicyloyl-β-D-glucose and glucosyloxybenzoic acid show a downward trend. Clearly, heating and sunlight can induce various chemical transformations of phenolic acids. These transformations can include decomposition, esterification reactions, rearrangement and isomerization processes. Given the substantial heating and sunlight in these steps, the content of phenolic compounds can be significantly affected. Phenolic compounds are often organic intermediates, and their involvement in subsequent chemical reactions can further impact their content. Furthermore, we observed that 24 compounds (Table S1) were exclusively detected in the processed groups, indicating that the heating and sunlight processes led to the modification of these compounds. Among these compounds were

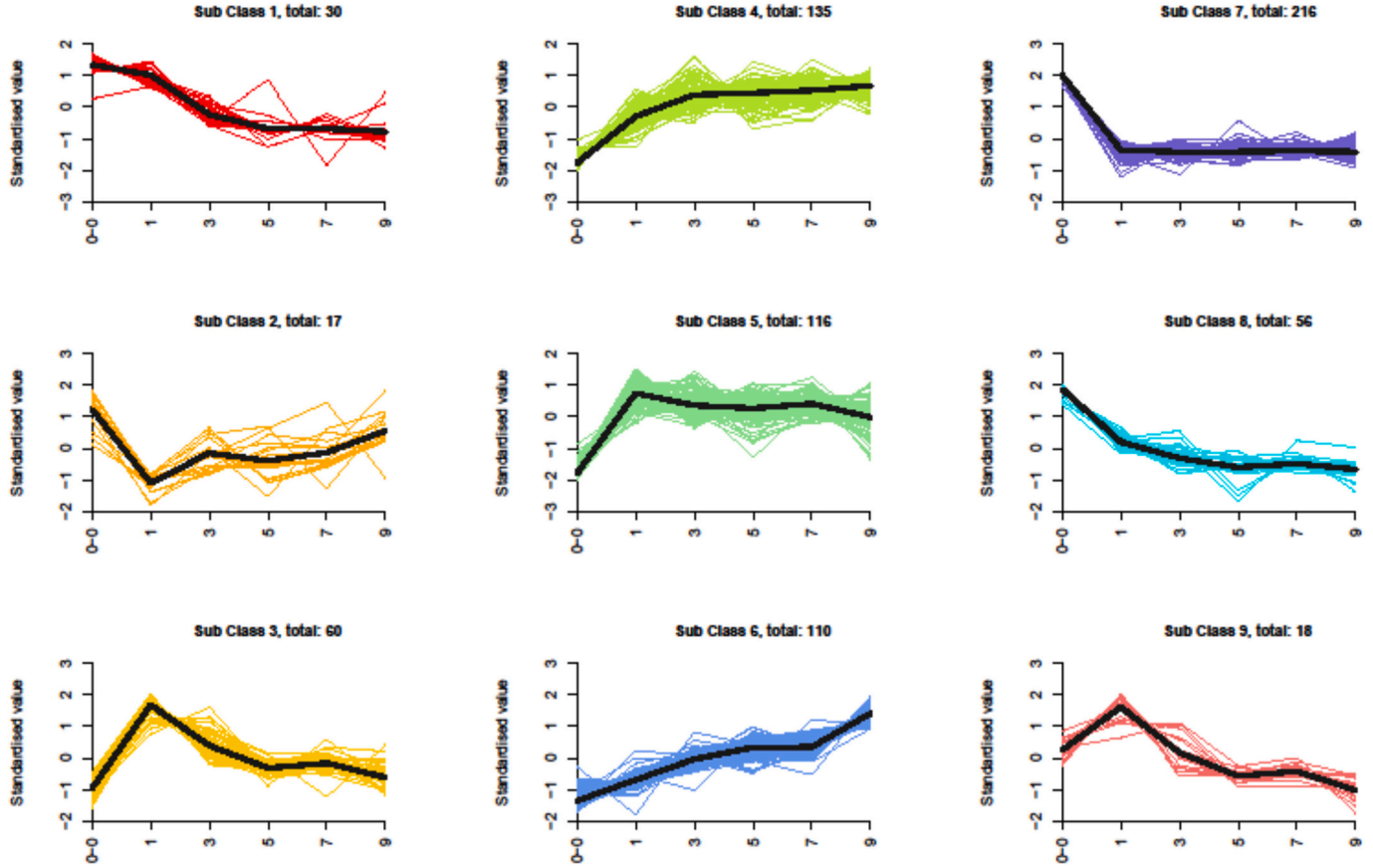

Fig. 3. K-means clustering groups of the differential metabolites of original group and the processed groups. Y axis: the standardized content of per metabolite; X axis: different processed groups.

pyrogallol, brevifolin carboxylic acid, ethyl caffeate, 4-aminosalicylic acid, phloroglucinol, veratric acid, caftaric acid and digallic acid.

3.3.2. *Organic acids*

Many common organic acids, including carboxylic acids, are known to exhibit thermal instability, making the steaming and dying processes critical determinants of their content. Among the top 20 compounds (Fig. 4) ranked by FC in different group comparisons, malonic acid demonstrated a downtrend, while mevalonic acid, citraconic acid, 4-hydroxy-2-oxoglutaric acid, 2-hydroxyglutaric acid, 5-hydroxymethyl-2-furancarboxylic acid, and 3-hydroxybutyric exhibited an uptrend. The proportion of organic acids was higher in the processed groups compared to the original groups. Additionally, 17 compounds (Table S1) were exclusively detected in the processed groups, including 3-hydroxybutyric acid, acetoxyacetic acid , citraconic acid , mevalonic acid , ethylmalonic acid , jasmonic acid , 2-oxovaleric acid, succinic semialdehyde and phenylpyruvic acid. The content of these components generally increases with an increase in processing cycles. Furthermore, the content of other components with significant changes, such as abscisic acid, fumaric acid, tranexamic acid, and 2-oxovaleric acid, exhibited a gradually increase with an increase in processing cycles.

3.3.3. *Amino acids and their derivatives*

In the top 20 compounds (Fig. 4) exhibiting the highest FCs across various group comparisons, there is a consistent decrease in content observed with an increase in processing cycles. Notable examples include dencichin, L-tryptophan, L-histidine and N-α-acetyl-L-ornithine. Similarly, several other compounds, such as *L*-phenylalanine, oxiglutatione, L-glutamic acid, L-cyclopentylglycine, L-asparagine and L-tyrosin, show a parallel declining trend, suggesting potential involvement in the Maillard reaction. For instance, we have detected an important Maillard reaction product, 5-hydroxymaltol. The content of 5-hydroxymaltol significantly increased after the first processing cycle. We simultaneously detected a decrease in maltose content. The reaction could be the Maillard reaction occurring between maltose and glutamic acid, and aspartic acid (Du et al., 2012). Conversely, certain components exhibit an initial increase in content following the initial processing, followed by a gradual decline with the subsequent processing cycles. Noteworthy instances include L-seryl- L-isoleucine,γ-glutamyl- L-valine, and γ-glutamyltyrosine. Additionally, five compounds, namely cyclo(Tyr-Ala), cyclo(Val-Ala), jasmonoyl-L-isoleucine, cyclo(Pro-Pro) and cyclo(Phe-Glu), were exclusively identified in the processed groups.

3.3.4. *Flavonoids*

Flavonoids play a crucial role in determining the antioxidant capacity of longan fruit, thereby significantly influencing their overall antioxidant properties (Zhang et al., 2018). In our study, among the top 20 compounds (Fig. 4) exhibiting with the highest FCs across various group comparisons, including cynaroside, luteolin-7,3′-di-O-glucoside, luteolin-7-O-gentiobioside and kaempferol-3,7-O-diglucoside, the contents of these components decreased during processing, followed by a gradual decline with subsequent processing cycles. Noteworthy examples include quercetin-3-O-(2″-O-galloyl)arabinoside, quercetin-3-O-rutinoside (rutin), quercetin-7-O-rutinoside, quercetin-3,4′-dimethyl ether, 3,4′-dihydroxyflavone, luteolin-3′-O-glucoside*, quercetin-3-O-glucoside-7-O-rhamnoside, kaempferol-3-O-glucoside-7-O-rhamnoside* and isorhamnetin-3-O-neohesperidoside*. Our findings align with those of Liao et al. (2022), who observed a significant decrease in the total flavonoid content of black soybeans following steaming and sun-drying treatments. Furthermore, 18 compounds (Table S1), such as quercetin-3,4′-dimethyl ether, luteolin-3′-O-glucoside*, hispidulin, jaceosidin, neodiosmin and tricin-7-O-glucoside, were exclusively

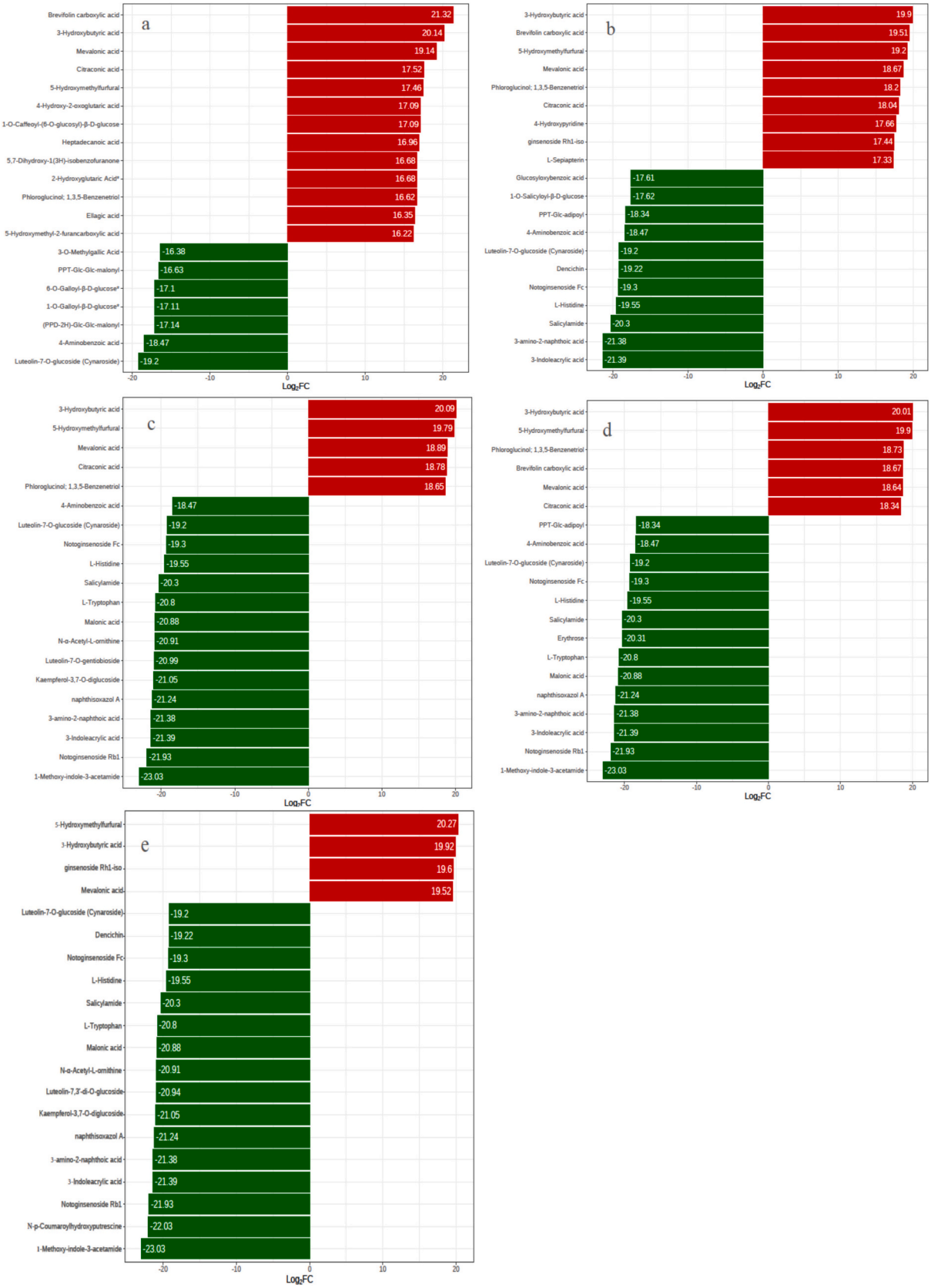

Fig. 4. Top 20 metabolites with the highest fold changes in each group comparison, red indicates up-regulated metabolites, while green indicates down-regulated metabolites. a.0 vs. 1, b. 0 vs. 3, c.0 vs. 5, d.0 vs. 7, e.0 vs. 9. (For interpretation of the references to colour in this figure legend, the reader is referred to the web version of this article.)

detected in the processed groups.

3.3.5. Lipids

The content of components showing higher FC values gradually decreases with an increase in processing cycles, exemplified by heptadecanoic acid. D-sphingosine, 9,16-dihydroxypalmitic acid, heptadecanoic acid, LysoPC 19:0, LysoPC 19:3 and LysoPC 10:0 were only detected in the processed groups.

3.3.6. Saccharides

The contents of D-glucose and D-fructose exhibited an upward trend through the processing stages. In contrast, the content of D-sucrose showed a decreasing trend during the processing, likely due to their hydrolysis into D-glucose and D-fructose during the steaming process. This hydrolysis reaction cleaves the glycosidic bond, resulting in the conversion of sucrose into glucose and fructose, which are more easily absorbed by the body. Additionally, 3-methyl-1-pentanol and maltotriose were exclusively found in the processed groups.

3.3.7. Terpenoids

Among the top 20 compounds (Fig. 4) exhibiting with the highest FCs across various group comparisons, specifically (PPD-2H)-Glc-Glc-malonyl, PPT-Glc-Glc-malonyl, notoginsenoside Fc, notoginsenoside Rb1 and PPT-Glc-adipoyl, showed a decreasing trend. Conversely, ginsenoside Rh1-iso showed an increasing trend. Furthermore, (PPD-2H)-Rha-Glc-acetyl, ginsenoside Rg7/Ib, Rh19, Rk3, Rh17, F5, ISO-ginsenoside F1, pomolic acid, Rh1-iso, (PPD-2H)-Glc-Rha, blumenol C, betulin, sanchinoside B1, β-amyrone, Rh3, Rh2, PPT-Rha-Glc-acetyl, Rs3, Rk1, PPT-acetyl-Glc-Rha, 11-keto-ursolic acid, isonotoginsenoside T5* and notoginsenoside T5*, were exclusively detected in the processed groups (Table S1).

3.3.8. Tannins

Longan fruit is rich in water-soluble tannins, such as ellagic acid, which have garnered considerable attention for their biological activities. Ellagic acid has been noted for its potential in normalising lipid metabolism and lipidemic profile, as well as regulating proinflammatory mediators such as IL-6, IL-1β and TNF-α (Gupta et al., 2021). Similarly, strictinin has been demonstrated to possess biological activity against the influenza virus (Saha et al., 2010). In our study, the total tannin content in the processed groups surpassed that of the original group. Notably, the tannin content increased after the initial treatment, but decreased with prolonged treatment time. Identified tannins included strictinin, ellagic acid, 3-*O*-methylellagic acid, ellagic acid-4-O-rhamnoside, 3,3'-*O*-dimethylellagic acid, and ellagic acid-4-O-xyloside. These findings indicate that while the process of steaming and drying enhances tannin content, prolonged processing durations have an opposite effect. Steaming not only causes tannins to leach out, but also induces chemical alterations in the tannin structures themselves.

3.3.9. Alkaloids

Alkaloids exhibit a wide range of effects on the human body, spanning from medicinal to toxic, contingent upon their type and concentration. In our study, we observed that the content of the components with the highest FC values (top 20) in different group comparisons decreased with an increase in processing cycles. Notably, alkaloids such as N-p-coumaroylhydroxyputrescine, 1-methoxy-indole-3-acetamide, 3-indoleacrylic acid, salicylamide, naphthisoxazol A, and 3-amino-2-naphthoic acid demonstrated this decreasing trend. We attribute this phenomenon to the hydrolysis and decomposition of these alkaloids during the steaming and sun-drying processes. Additionally, we exclusively detected seven compounds: 1-[1-O-5(3,4-methylenedioxy-phenyl)-2E,4E-pentadienyl]-pyrrolidine, acetylpyrazine, carbazole-3-carboxylic acid, 2-amino-4-dihydroxy octadecyl galactoside, 4-hydroxy-pyridine, 3-hydroxypyridine and 7-hydroxy-β-carboline-1-propionic acid in the processed groups (Table S1). These findings shed light on the impact of processing on the composition of alkaloids in these samples.

3.3.10. Nucleotides and derivatives

The content of components with higher FC values increases after the initial processing and subsequently decreases gradually with successive processing cycles. Examples of such compounds include 8-hydroxyguanosine, 2′-*O*-methyladenosine, guanosine 3′,5′-cyclic monophosphate, adenosine, 2′-deoxycytidine, vidarabine and cytidine. Furthermore, six compounds(Table S1), namely L-sepiapterin, 3-methylxanthine, 1-methyladenosine, 2′-deoxycytidine-5′-monophosphate, 8-hydroxyguanosine and thymine, were exclusively detected in the processed groups.

3.3.11. Lignans and coumarins

The content of components with higher FC values gradually decreases with an increase in processing cycles, as observed with compounds such as 3,4-methylenedioxy cinnamyl alcohol, isolariciresinol, guaiacylglycerol, β-coniferyl ether, syringaresinol-4′-O-(6″-acetyl) glucoside, clemastanin A, secoisolariciresinol 4-O-glucoside and 5′-methoxyisolariciresinol-9′-O-glucoside. Additionally, five compounds (Table S1), such as coumarin, syringaresinol, 7-methoxycoumarin, fraxidin and 7,8-dihydroxy-4-methylcoumarin, were exclusively detected in the processed groups.

3.4. Network pharmacology analysis

3.4.1. Prediction of active ingredients and core targets

Active ingredients from longan pulp and American ginseng were screened using the Traditional Chinese Medicine System Pharmacological database and analysis platform (TCMSP), the Integrative Pharmacology-based Research Platform of Traditional Chinese Medicine (TCMIP v2.0) and the Encyclopaedia of Traditional Chinese Medicine. Only ingredients meeting the criteria of oral bioavailability $\geq$30% and drug-like properties $\geq$0.18 were selected. The effective components obtained from longan pulp and American ginseng are detailed in Table S2.

The SwissTargetPrediction database was used to predict the target points of these components. A total of 125 target points were identified for longan pulp and 183 target points for American ginseng. After removing duplicates, 199 unique target points remained. Disease targets were identified through screening in the OMIM and GeneCards databases. Venn analysis revealed 96 targets shared between EF and disease (Fig. S5). To evaluate the targets associated with enhancing energy (qi) and blood nourishment by longan pulp and American ginseng, the STRING database and Cytoscape software were used. Finally, 18 core targets were identified (Table S3). These 18 target points were considered the core targets for Yuling paste associated with treating ischaemic qi deficiency.

Upon comparing and screening all acquired active ingredients with all differential metabolites, we identified 46 ingredients, as detailed in Table S4. Subsequently, ingredients lacking target information were excluded, and similar ingredients were classified, resulting in a total of 24 overlapping active ingredients, comprising 10 upregulated and 14 downregulated ingredients. The specific ingredients are detailed in Table 1.

Oleanolic acid, a natural pentacyclic triterpenoid compound found in various plants such as *Ligustrum lucidum*, olives and various fruit plants (Jäger, Trojan, Kopp, Laszczyk, & Scheffler, 2009; Xia et al., 2011), has been extensively for its pharmacological activities, including antioxidant, anticancer and anti-inflammatory effects (Wang et al., 2013). In our study, oleanolic acid was categoried as sub-class 6 based on K-means clustering (Fig. 3). Interestingly, as depicted in Fig. S4, the content of oleanolic acid increased with the processing cycle, enhancing by 26 times after treatment. This observed increase could be attributed to the breakdown of cell structures or alterations in chemical compositions during the processing, facilitating the release of bound or insoluble

Table 1
A list of 24 main active ingredients.

Name	CAS No.	Class	Targets	Trend
Chrysosplenetin	603-56-5	Flavonoids	16	up
Galacturonic acid	14,982-50-4	Saccharides	5	up
Ginsenoside rh2	78,214-33-2	Terpenoids	11	up
Oleanolic acid	508-02-1	Terpenoids	4	up
Quercetin	117-39-5	Flavonoids	29	up
Dimethyl phthalate	131-11-3	Phenolic acids	3	up
Gallic acid	149-91-7	Phenolic acids	3	up
Glucose	50-99-7	Saccharides	13	up
Pulegone	89-82-7	Flavonoids	2	up
Tartaric Acid	87-69-4	Organic acids	8	up
Caprylic acid	124-07-2	Organic acids	24	Down
Vitamin b5	79-83-4	Vitamin	6	Down
Narirutin	14,259-46-2	Flavonoids	1	Down
Hesperidin	520-26-3	Flavonoids	5	Down
Phlorizin	60-81-1	Flavonoids	3	Down
Naringin	10,236-47-2	Flavonoids	5	Down
Naringenin	480-41-1	Flavonoids	15	Down
Sucrose	57-50-1	Saccharides	35	Down
Adenine	73-24-5	Nucleotides and derivatives	9	Down
Rutin	153-18-4	Flavonoids	8	Down
Choline	62-49-7	Lipids	7	Down
Isoeugenol	97-54-1	Phenolic acids	2	Down
Hexanoic acid	142-62-1	Organic acids	2	Down
Nonanoic acid	112-05-0	Organic acids	1	Down

oleanolic acid. Moreover, oleanolic acid-GlurA and Oleanolic acid-3-O-xylosyl(1 → 3)glucuronide, classified into subs 7 and 5 based on K-means clustering, respectively, showed a decrease in content as the processing cycle increased. Therefore, our findings suggest that steaming and drying treatments are conducive to increasing oleanolic acid levels.

Gallic acid, a natural phenolic acid, boasts a plethora of physiological functions, including its well-documented antioxidant and anti-inflammatory properties (Dhingra, Dhingra, Chadha, Singh, & Karan, 2014; Lone, Rehman, & Bhat, 2017). Numerous studies have highlighted the anti-inflammatory activity of phenols, attributing their property not only to their antioxidant capacity but also to the modulation of inflammatory mediators, namely cytokines and proinflammatory enzymes such as inducible nitric oxide synthase and cyclooxygenase (Costa, Francisco, C Lopes, T Cruz, & T Batista, 2012). In our study, gallic acid was categorized as sub-class 5 based on K-means clustering. As depicted in Fig. S4, the content of gallic acid exhibited an initial increase during the first three processing cycles, followed by a gradual decrease in the subsequent processing. Notably, the content of gallic acid peaked after the third treatment, increased by 36 times relative to the original group. Following the final treatment, the gallic acid content was still 16 times higher that of the original group. Digallic acid, catogoried as sub-class 6, also exhibited an increasing trend in content during processing. The content levels of these two components after processing surpassed those observed before processing. During the steaming process, gallic acid can be liberated from the food matrix as steam could disrupt plant cell structures. Higher temperatures and prolonged steaming durations result in a greater release of gallic acid. However, it's noteworthy that gallic acid exhibits better solubility in hot water, and prolonged steaming may result in the loss of gallic acid along with the water vapour.

Quercetin, a flavonoid compound derived from plants and widely utilized in traditional Chinese medicine, boasts various pharmacological properties, including anti-cancer and hold promise in treating cardiovascular and inflammatory ailments (Kleemann et al., 2011). Quercetin-3-O-sophoroside (baimaside) has been linked to neuroprotective effects by modulating the cholinergic system (Shen, Zheng, Chen, Huang, & Shi, 2021). In our study, the baimaside content dropped to zero after the initial treatment, with no subsequent increase. Furthermore, the quercetin derivative, quercetin-3-o-(2″-o-galloyl) arabinoside, categorized as sub-class 3 based on K-means clustering, initially increased in content after the first treatment before subsequently decreasing, although the overall content remained higher than that of the original group. Conversely, the content of quercetin-3-O-rhamnosyl(1 → 2) arabinoside and quercetin-3-O-sophoroside decreased after the first processing and then remained unchanged. Arowoogun et al. (2021) found the anti-inflammatory effects of quercetin-3-O-rutinoside (rutin), demonstrating reductions in myeloperoxidase and nitric oxide activity levels, along with a significant decrease in cyclooxygenase-2 concentration. Our results (Fig. S4) revealed that the first treatment yielded the highest rutin content, peaking at 12.6 times that of the untreated group, before gradually declining to the level observed in the untreated group. In summary, our findings indicate that short-term treatment is beneficial for quercetin and its derivatives, whereas prolonged treatment may lead to a significant reduction in their content.

Naringenin, a flavanone, exhibits anti-inflammatory and anti-infective properties. Naringenin-7-O-glucoside has been demonstrated to protect against cardiomyocyte apoptosis (Han et al., 2008). Tangeretin could induce apoptosis via intrinsic and extrinsic pathways and arrest the cell cycle (Raza, Luqman, & Meena, 2020). In the current study, the naringenin-4′-O-glucoside content decreased by 90% (Fig. S4) after the first treatment, followed by a slight increase.

Galacturonic acid, a monosaccharide found in pectin, has been shown in previous studies to reduce intestinal mucosal permeability and inflammatory response in functional dyspepsia rats by downregulating TLR2, TLR4 and NF-κB (Wu et al., 2021). In the current study, the D-galacturonic acid content gradually increases with an increase in the number of processing cycles, eventually reaching 11 times (Fig. S4) that of the original group. Steaming may facilitate the breakdown of plant cell walls and pectin, releasing more galacturonic acid from the insoluble fibre structures.

Ginsenoside, a relevant active ingredient in ginseng, has been extensively studied for its biological therapeutic activities (Kim et al., 2014). Previous studies have shown that certain treatments, such as steaming, may enhance American ginseng's effects, including its anti-cancer activities (Shibata, 2001). Some ordinary ginsenosides undergo conversion to rare ginsenosides under heating conditions. High-temperature treatment promotes oxidation, hydrolysis, isomerisation and other rapid thermochemical reactions of these substances (Zheng et al., 2017). In the present study, mainly ginsenosides (Re, Rd, Re5, Rg1, Rh15, Ro, ST2, ST3, Rh14, Rh17, Rh4, Rf1, Rb3) showed a downward trend during the processing. Additionally, ginsenosides (Rg7, Rf1, Rk3, Rh17, R-Rg3, Rh3, Rg4, Rh2, Rk1, Rk2*, Rg6, Rh19, F1, 2, Rs3, F5, Rg2) showed an increasing trend. Certain ginsenosides (Rk3, Rg7/Ib, Rh19, Rs3, Rk1, F5, Rh17, Rh3, Rh2), (PPD-2H)-Rha-Glc-acetyl, ISO-ginsenoside F1, Rh1-iso, (PPD-2H)-Glc-Rha, sanchinoside B1, PPT-Rha-Glc-acetyl, PPT-acetyl-Glc-Rha, isonotoginsenoside T5* and notoginsenoside T5* were exclusively detected in the processed groups. It is interesting to note that the content of ginsenoside Rh2 (Fig. S4) increase significantly after the processing, reaching its peak during the third processing cycle.

Pantothenic acid (vitamin B5) and nicotinamide levels decreased significantly after the first three cycles and became non-detectable thereafter, with vitamin B5 content decreasing by 99% (Fig. S4) after the third treatment. Riboflavin (vitamin B2) and orotic acid (vitamin B13) initially increased and then decreased, but their total content remained higher than that of the original group.

Adenosine serves as a neuromodulator, regulating neuronal activity in the central nervous system and playing multiple physiological functions, including promoting or maintaining sleep, regulating alertness, and modulating local neuronal excitability (Dunwiddie & Masino, 2001). In this study, the content of adenosine increased to 2.4 times

(Fig. S4) that of the original group after the first treatment and then gradually decreased.

Choline, an essential nutrient and a vital component of cell membranes (Zeisel & Da Costa, 2009), increased in content as the processing cycle progressed. Specifically, the content of choline increased with each treatments, eventually reaching 1.7 times (Fig. S4) that of the original group.

3.4.2. KEGG pathway enrichment analysis

In order to gain further insights into the mechanisms underlying the 'invigorating qi and nourishing blood' activity of Yuling paste, we conducted GO analysis on the differential metabolites, exploring for the targets of 10 upregulated components in the TCMSP and Swiss Target Prediction databases. Resulting in a total of 81 unique target genes after removing duplicates. Similarly, we identified 105 target genes from 14 downregulated components. Subsequently, KEGG pathway analysis was conducted on the upregulated genes using the DAVID database, yielding 93 enriched pathways. These pathways were ranked based on their *P*-values and visualised in a bubble plot. The top 20 pathways identified in Fig. 5a are as follow: pathways in cancer, lipid and atherosclerosis, IL-17 signalling pathway, Yersinia infection, Kaposi sarcoma-associated herpesvirus infection, human cytomegalovirus infection, oestrogen signalling pathway, measles, C-type lectin receptor signalling pathway, shigellosis, salmonella infection, toxoplasmosis, TNF signalling pathway, leishmaniasis, hepatitis B, influenza A, osteoclast differentiation and tuberculosis.

Similarly, KEGG analysis of the downregulated genes revealted 77 enriched pathways. The top 20 pathways, arranged by P-values, are

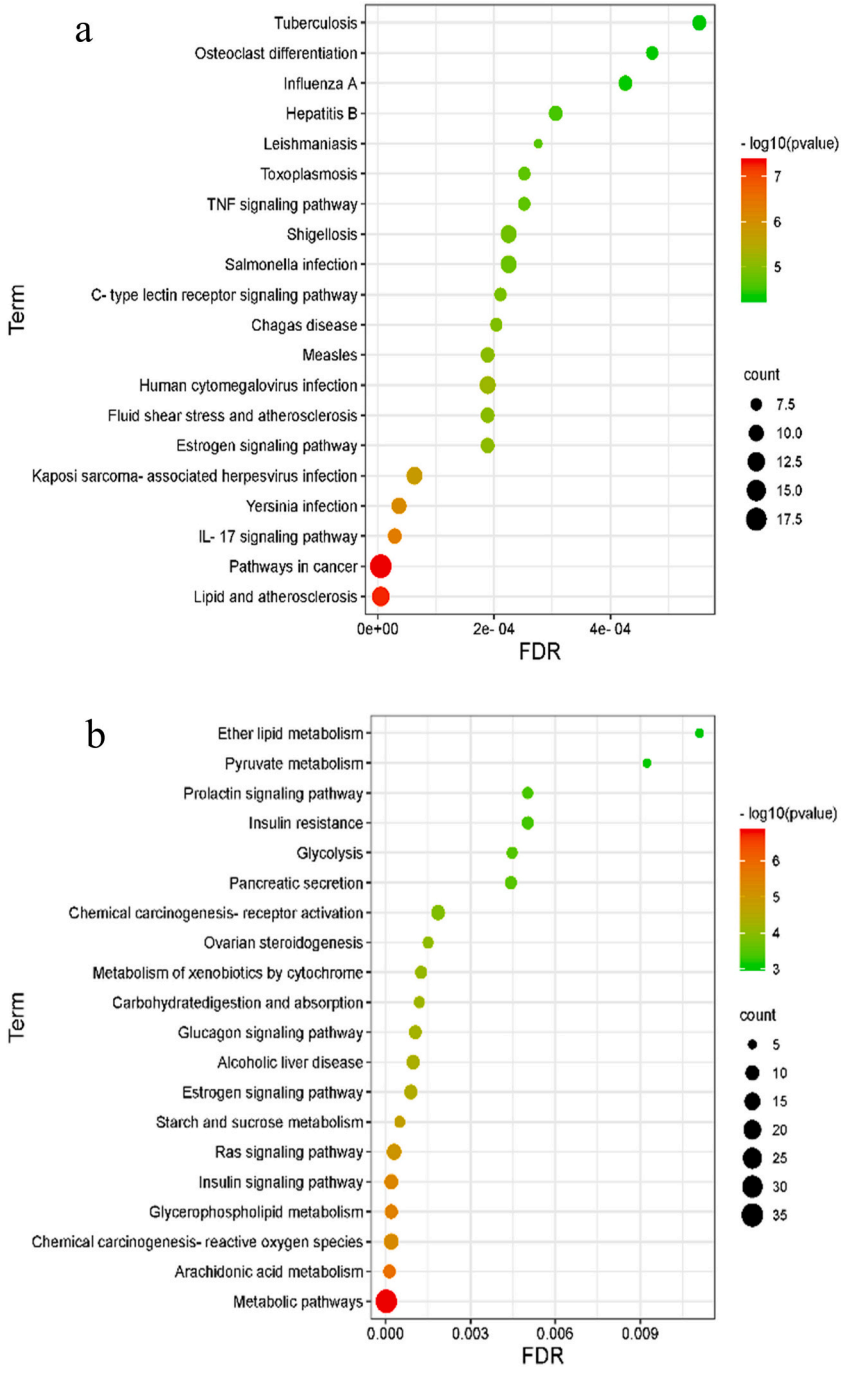

Fig. 5. KEGG pathway enrichment analysis of the top 20 pathways. a. Upregulated Genes. b. Downregulated Genes.

shown in Fig. 5b: metabolic pathways, arachidonic acid metabolism, glycerophospholipid metabolism, insulin signalling pathway, chemical carcinogenesis—ROS, ras signalling pathway, starch and sucrose metabolism, oestrogen signalling pathway, alcoholic liver disease, glucagon signalling pathway, carbohydrate digestion and absorption, metabolism of xenobiotics by cytochrome, ovarian steroidogenesis, chemical carcinogenesis-receptor activation, pancreatic secretion, glycolysis, prolactin signalling pathway, insulin resistance, pyruvate metabolism and ether lipid metabolism.

Further enrichment analysis was performed on the upregulated and downregulated genes, together with the intersection of all identified genes. It was observed that the pathways associated with the active components in longan and American ginseng were influenced after the processing. Specifically, the upregulated components impact pathways such as 'inhibition of the IL-17 signalling pathway', 'enhancement of the oestrogen signalling pathway', 'increased lipid metabolism', 'inhibition of atherosclerosis pathways' and 'enhancement of osteoclast differentiation pathways', which are strengthened after the processing. Conversely, the downregulated components were linked to pathways such as 'inhibition of cGMP-PKG pathway activation' and 'reduced sensitivity of chemical carcinogenesis receptors', which are weakened after the processing. These changes in pathways collectively suggest an overall effect of promoting blood circulation, reducing inflammation and exhibiting anti-viral and anti-tumour properties.

4. Conclusions

The present study utilized widely targeted metabolomic analysis to investigate alterations in metabolites throughout the processing of 'Yuling paste', involving nine steaming and nine sun-drying cycles. A total of 758 differential metabolites were identified, including amino acids, flavonoids, phenolic acids, organic acids, lipids, triterpenes, nucleotides, tannins, alkaloids, organic acids, lignans, coumarins, etc. After processing, 10 key active ingredients exhibited an upwards trend in content, while 14 ingredients displayed a declining trend. KEGG analyses unveiled that the targets of 'Yuling paste' exerting 'nourishing qi and blood' predominantly enriched in the pathways related to the 'inhibition of the IL-17 signalling pathway', 'enhancement of the oestrogen signalling pathway', 'increased lipid metabolism', 'inhibition of atherosclerosis pathways' and 'enhancement of osteoclast differentiation pathways'. Conversely, these targets were attenuated in the pathways associated with the 'inhibition of cGMP-PKG pathway activation' and 'reduced sensitivity of chemical carcinogenesis receptors'. This study has provided preliminary insights into the differential ingredients, potential pharmacological ingredients and mechanisms underlying the 'nourishing qi and blood' effects of Yuling paste. Functional assessment, as well as in-depth studies on its health effects on humans, are also worthy of future investigation.

CRediT authorship contribution statement

Yue E: Writing – original draft, Methodology, Formal analysis, Data curation, Conceptualization. **Weimiao Li:** Writing – original draft, Investigation, Formal analysis. **Hongbin Guo:** Data curation. **Xianman Zhang:** Writing – review & editing. **Qinggele Caiyin:** Writing – review & editing, Supervision, Project administration, Funding acquisition. **Yi Yuan:** Writing – review & editing, Validation.

Declaration of competing interest

The authors declare that they have no known competing financial interests or personal relationships that could have appeared to influence the work reported in this paper.

Data availability

No data was used for the research described in the article.

Acknowledgment

Thanks to the Shaoxing People's Government for a supporting of her post-doctoral research. This work was supported by the National Key Research and Development Program of China (2020YFA0906800).

Appendix A. Supplementary data

Supplementary data to this article can be found online at https://doi.org/10.1016/j.fochx.2024.101668.

References

Arowoogun, J., Akanni, O. O., Adefisan, A. O., Owumi, S. E., Tijani, A. S., & Adaramoye, O. A. (2021). Rutin ameliorates copper sulfate-induced brain damage via antioxidative and anti-inflammatory activities in rats. *Journal of Biochemical and Molecular Toxicology, 35*(1), Article e22623.

Bai, Y., Zhou, Y., Li, X., Zhang, R., Huang, F., Fan, B., … Zhang, M. (2023). Longan pulp polysaccharides regulate gut microbiota and metabolites to protect intestinal epithelial barrier. *Food Chemistry, 422*, Article 136225.

Cheng, R., Liao, X., Addou, A. M., Qian, J., Wang, S., Cheng, Z., … Huang, J. (2021). Effects of "nine steaming nine sun-drying" on proximate composition, oil properties and volatile compounds of black sesame seeds. *Food Chemistry, 344*, Article 128577.

Corbit, R., Ebbs, S., King, M. L., & Murphy, L. L. (2006). The influence of lead and arsenite on the inhibition of human breast cancer MCF-7 cell proliferation by American ginseng root (*Panax quinquefolius* L.). *Life Sciences, 78*(12), 1336–1340.

Costa, G., Francisco, V., C Lopes, M., T Cruz, M., & T Batista, M. (2012). Intracellular signaling pathways modulated by phenolic compounds: Application for new anti-inflammatory drugs discovery. *Current Medicinal Chemistry, 19*(18), 2876–2900.

Dhingra, M. S., Dhingra, S., Chadha, R., Singh, T., & Karan, M. (2014). Design, synthesis, physicochemical, and pharmacological evaluation of gallic acid esters as non-ulcerogenic and gastroprotective anti-inflammatory agents. *Medicinal Chemistry Research, 23*, 4771–4788.

Du, Q. Q., Liu, S. Y., Xu, R. F., Li, M., Song, F. R., & Liu, Z. Q. (2012). Studies on structures and activities of initial Maillard reaction products by electrospray ionisation mass spectrometry combined with liquid chromatography in processing of red ginseng. *Food Chemistry, 135*(2), 832–838.

Dunwiddie, T. V., & Masino, S. A. (2001). The role and regulation of adenosine in the central nervous system. *Annual Review of Neuroscience, 24*(1), 31–55.

Gong, P. Y., Guo, Y. J., Tian, Y. S., Gu, L. F., Qi, J., & Yu, B. Y. (2021). Reverse tracing anti-thrombotic active ingredients from dried Rehmannia Radix based on multidimensional spectrum-effect relationship analysis of steaming and drying for nine cycles. *Journal of Ethnopharmacology, 276*, Article 114177.

Gupta, A., Singh, A. K., Kumar, R., Jamieson, S., Pandey, A. K., & Bishayee, A. (2021). Neuroprotective potential of ellagic acid: A critical review. *Advances in Nutrition, 12*(4), 1211–1238.

Han, X., Pan, J., Ren, D., Cheng, Y., Fan, P., & Lou, H. (2008). Naringenin-7-O-glucoside protects against doxorubicin-induced toxicity in H9c2 cardiomyocytes by induction of endogenous antioxidant enzymes. *Food and Chemical Toxicology, 46*(9), 3140–3146.

Jäger, S., Trojan, H., Kopp, T., Laszczyk, M. N., & Scheffler, A. (2009). Pentacyclic triterpene distribution in various plants–rich sources for a new group of multi-potent plant extracts. *Molecules, 14*(6), 2016–2031.

Kan, J., Velliquette, R. A., Grann, K., Burns, C. R., Scholten, J., Tian, F., … Gui, M. (2017). A novel botanical formula prevents diabetes by improving insulin resistance. *BMC Complementary and Alternative Medicine, 17*, 1–10.

Kiefer, D., & Pantuso, T. (2003). Panax ginseng. *American Family Physician, 68*(8), 1539–1542.

Kim, J., Ahn, H., Han, B. C., Lee, S. H., Cho, Y. W., Kim, C. H., … Lee, G. S. (2014). Korean red ginseng extracts inhibit NLRP3 and AIM2 inflammasome activation. *Immunology Letters, 158*(1–2), 143–150.

Kleemann, R., Verschuren, L., Morrison, M., Zadelaar, S., van Erk, M. J., Wielinga, P. Y., & Kooistra, T. (2011). Anti-inflammatory, anti-proliferative and anti-atherosclerotic effects of quercetin in human in vitro and in vivo models. *Atherosclerosis, 218*(1), 44–52.

Liao, X., Miao, Q., Yang, J., Olajide, T. M., Wang, S., Liu, H., & Huang, J. (2022). Changes in phenolic compounds and antioxidant activities of "nine steaming nine sun-drying" black soybeans before and after in vitro simulated gastrointestinal digestion. *Food Research International, 162*, Article 111960.

Lone, S. H., Rehman, S. U., & Bhat, K. A. (2017). Synthesis of gallic-acid-1-phenyl-1H-[1,2,3] triazol-4-yl methyl esters as effective antioxidants. *Drug Research, 11*(02), 111–118.

Raza, W., Luqman, S., & Meena, A. (2020). Prospects of tangeretin as a modulator of cancer targets/pathways. *Pharmacological Research, 161*, Article 105202.

Robards, K., Prenzler, P. D., Tucker, G., Swatsitang, P., & Glover, W. (1999). Phenolic compounds and their role in oxidative processes in fruits. *Food Chemistry, 66*(4), 401–436.

Saha, R. K., Takahashi, T., Kurebayashi, Y., Fukushima, K., Minami, A., Kinbara, N., … Suzuki, T. (2010). Antiviral effect of strictinin on influenza virus replication. *Antiviral Research, 88*(1), 10–18.

Shen, H., Zheng, Y., Chen, R., Huang, X., & Shi, G. (2021). Neuroprotective effects of quercetin 3-O-sophoroside from *Hibiscus rosa-sinensis* Linn. on scopolamine-induced amnesia in mice. *Journal of Functional Foods, 76*, Article 104291.

Shibata, S. (2001). Chemistry and cancer preventing activities of ginseng saponins and some related triterpenoid compounds. *Journal of Korean Medical Science, 16*(Suppl), S28–S37.

Shin, K., Guo, H., Cha, Y., Ban, Y. H., Seo, D. W., Choi, Y., … Kim, Y. B. (2016). Cereboost™, an American ginseng extract, improves cognitive function via up-regulation of choline acetyltransferase expression and neuroprotection. *Regulatory Toxicology and Pharmacology, 78*, 53–58.

Su, L. L., Li, X., Guo, Z. J., Xiao, X. Y., Chen, P., Zhang, J. B., … Lu, T. L. (2023). Effects of different steaming times on the composition, structure and immune activity of polygonatum polysaccharide. *Journal of Ethnopharmacology, 310*, Article 116351.

Sun, Y., Zhou, L., Shan, X., Zhao, T., Cui, M., Hao, W., & Wei, B. (2023). Untargeted components and in vivo metabolites analyses of Polygonatum under different processing times. *LWT, 173*, Article 114334.

Szczuka, D., Nowak, A., Zakłos-Szyda, M., Kochan, E., Szymańska, G., Motyl, I., & Blasiak, J. (2019). American ginseng (*Panax quinquefolium* L.) as a source of bioactive phytochemicals with pro-health properties. *Nutrients, 11*(5), 1041.

Tindall, H. D. (1994). Sapindaceous fruits: Botany and horticulture. *Horticultural Reviews, 16*, 143–196.

Wang, X., Liu, R., Zhang, W., Zhang, X., Liao, N., Wang, Z., … Hai, C. (2013). Oleanolic acid improves hepatic insulin resistance via antioxidant, hypolipidemic and anti-inflammatory effects. *Molecular and Cellular Endocrinology, 376*(1–2), 70–80.

Wu, Y. Y., Zhong, Z. S., Ye, Z. H., Zhang, W., He, G. H., Zheng, Y. F., & Huang, S. P. (2021). D-galacturonic acid ameliorates the intestinal mucosal permeability and inflammation of functional dyspepsia in rats. *Annals of Palliative Medicine, 10*(1), 53848–53548.

Xia, E. Q., Wang, B. W., Xu, X. R., Zhu, L., Song, Y., & Li, H. B. (2011). Microwave-assisted extraction of oleanolic acid and ursolic acid from Ligustrum lucidum Ait. *International Journal of Molecular Sciences, 12*(8), 5319–5329.

Yang, B., Jiang, Y., Shi, J., Chen, F., & Ashraf, M. (2011). Extraction and pharmacological properties of bioactive compounds from longan (*Dimocarpus longan* Lour.) fruit—A review. *Food Research International, 44*(7), 1837–1842.

Yu, L. (2020). Wang Shixiong's medicine career. *Chinese Medicine and Culture, 3*(4), 254–256.

Zeisel, S. H., & Da Costa, K. A. (2009). Choline: An essential nutrient for public health. *Nutrition Reviews, 67*(11), 615–623.

Zhang, R., Khan, S. A., Lin, Y., Guo, D., Pan, X., Liu, L., … Zhang, M. (2018). Phenolic profiles and cellular antioxidant activity of longan pulp of 24 representative Chinese cultivars. *International Journal of Food Properties, 21*(1), 746–759.

Zhang, X., Guo, S., Ho, C. T., & Bai, N. (2020a). Phytochemical constituents and biological activities of longan (*Dimocarpus longan* Lour.) fruit: A review. *Food Science and Human Wellness, 9*(2), 95–102.

Zhang, X., Guo, S., Ho, C. T., & Bai, N. (2020b). Phytochemical constituents and biological activities of longan (*Dimocarpus longan* Lour.) fruit: A review. *Food Science and Human Wellness, 9*(2), 95–102.

Zheng, M. M., Xu, F. X., Li, Y. J., Xi, X. Z., Cui, X. W., Han, C. C., & Zhang, X. L. (2017). Study on transformation of ginsenosides in different methods. *BioMed Research International, 2017*(1), 8601027.

Zhu, S., Liu, P., Wu, W., Li, D., Shang, E. X., Guo, S., … Duan, J. A. (2022). Multi-constituents variation in medicinal crops processing: Investigation of nine cycles of steam-sun drying as the processing method for the rhizome of Polygonatum cyrtonema. *Journal of Pharmaceutical and Biomedical Analysis, 209*, Article 114497.